Debye Lecture 7

Nanostructured Magnetic Materials for Biotechnology

C. B. Murray

Designing Nanoscale Materials

Lecture Series by 2004 Debye Institute Professor

Christopher B. Murray

IBM Research

Ornstein Laboratory 166

Office phone 253 2227

cbmurray@alum.mit.edu

Bind to Specific Cells

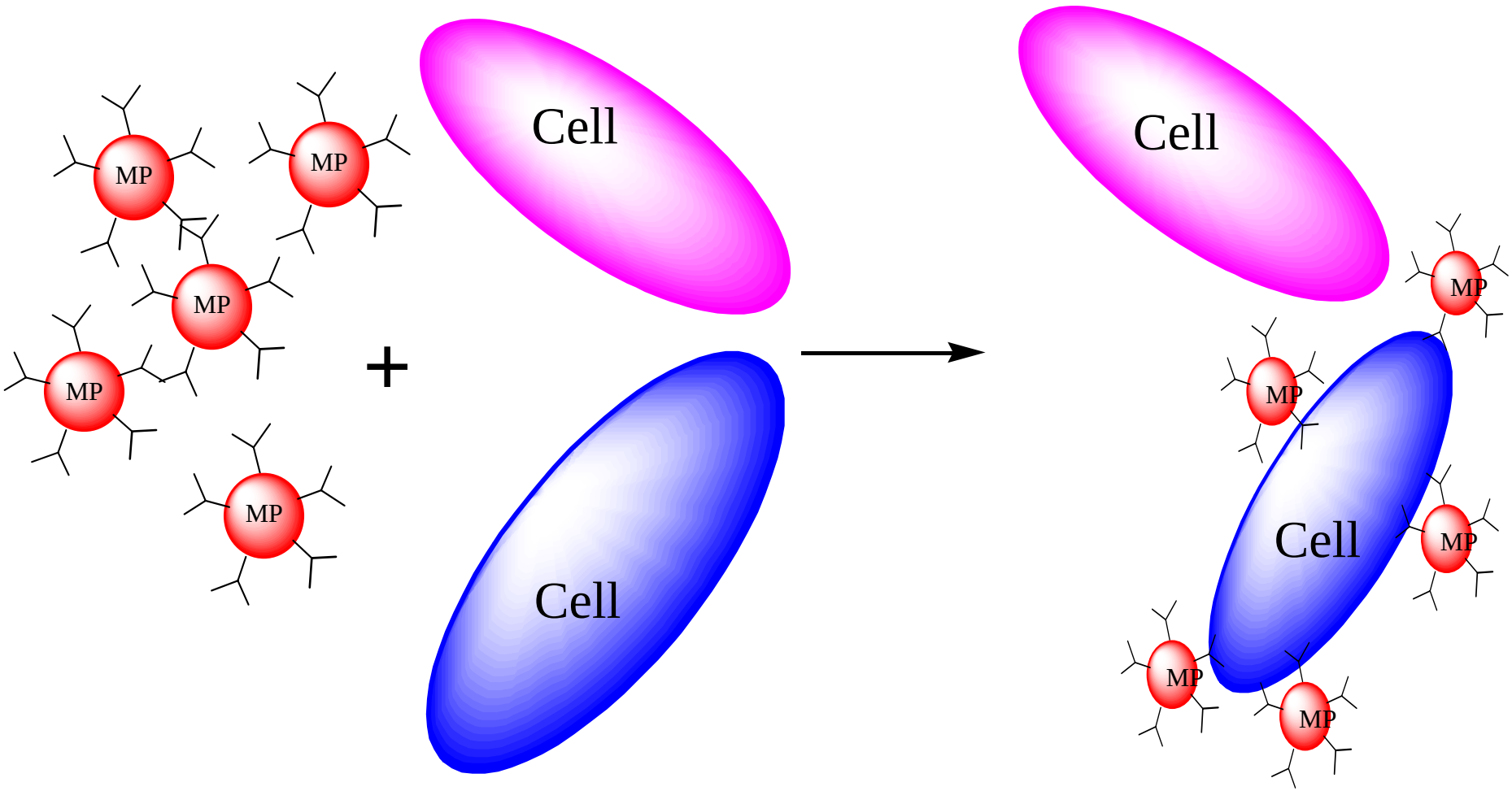

Uses for magnetically labeled cells

A: Cell sorting

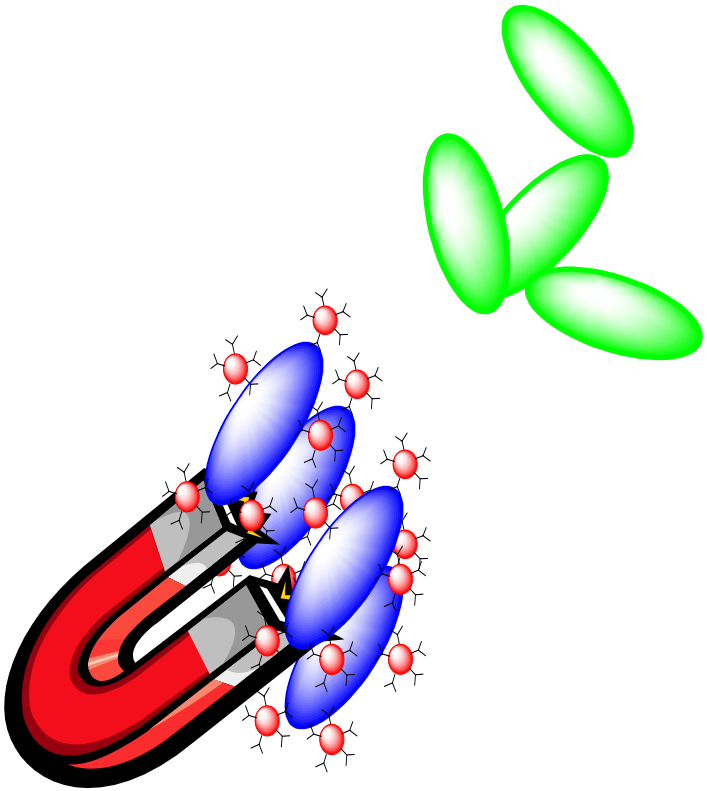

B: Magnetic Fluid Hyperthermia

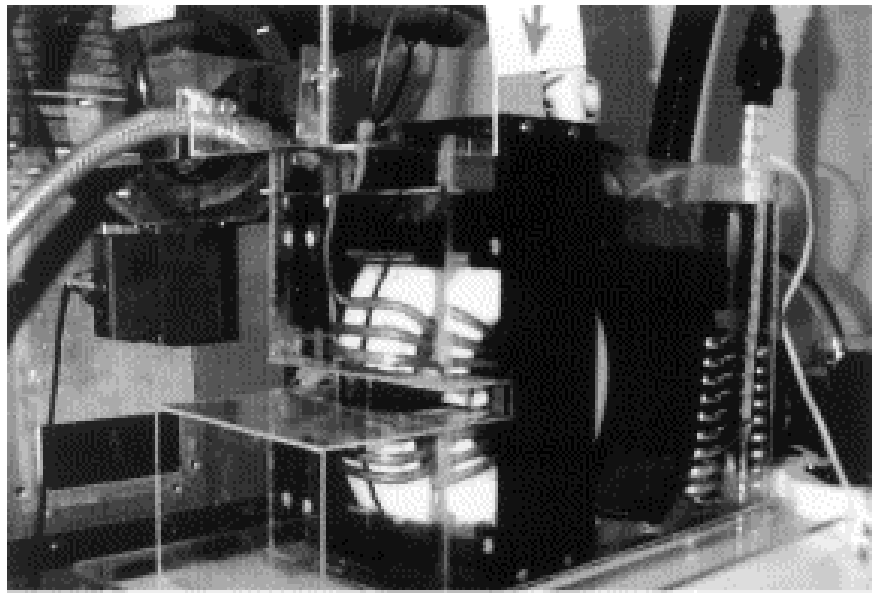

Jordan, A. et. al. J Magn Magn Mater, **201** (1999) 413-419

Roger, J.; et. al. Eur. Phys. J. AP **5**, 321-325 (1999)

Magnetic Fluid Hyperthermia (MFH)

- Also known as magnetocytolysis
- Inject fluid containing MP's into patient
- Use constant magnetic field to maneuver particles to desired location (tumor, for example)
- Expose area to oscillating magnetic field to cause extremely localized heating
- Prototype unit being built in Germany

Jordan, A. et. al. J Magn Magn Mater, **201** (1999) 413-419

Animal Test Results

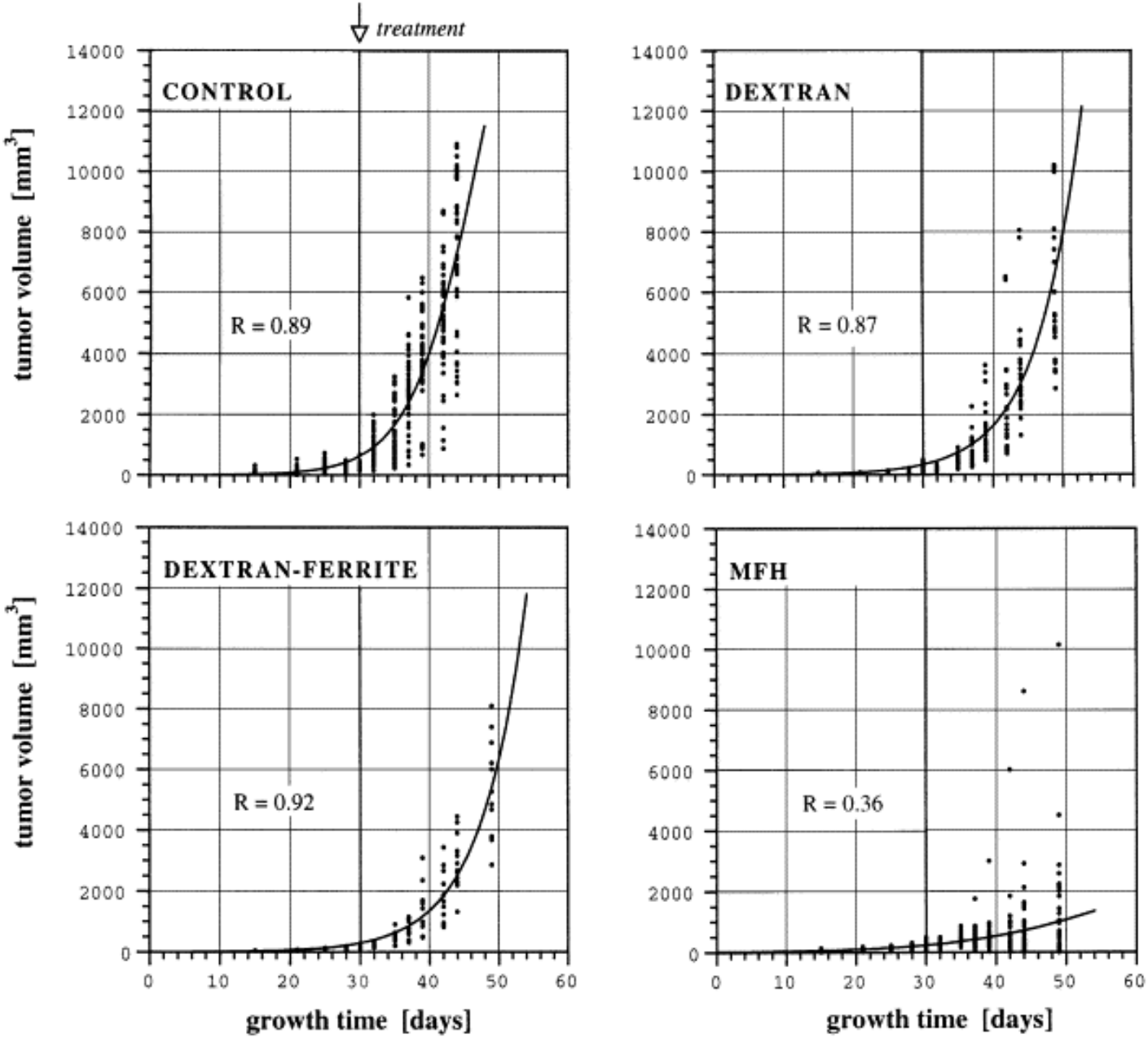

Jordan, A. et. al. J. Magn Magn Mater, 201 (1999) 413-419

Magnetic Nanoparticle MRI Contrast Agents.
Commercial names ferridex, combidex, Gastromark Etc
MRI Imaging agents are a potential 1B dollar market.

Real time imaging of Spleen Lesions

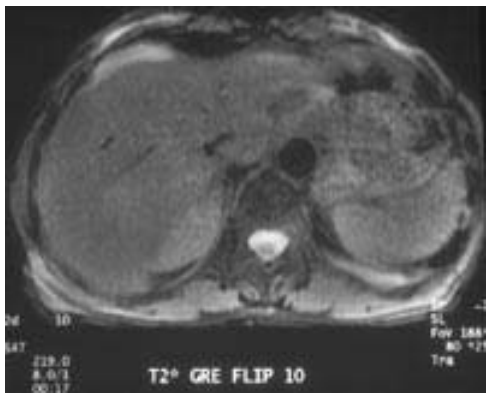

Without NP
Contrast agents

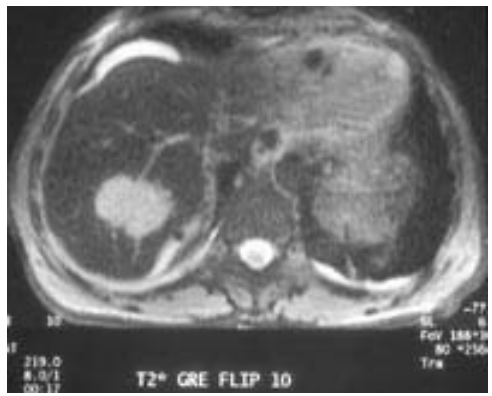

With NP Contrast
Agents.

BARC: The Bead ARray Counter

A microchip with an array of GMR field sensors.

1. Array ssDNA probes on chip
2. Protect with nonfouling PEG film
3. Capture complementary ssDNA in sample (biotinylated)
4. Inject streptavidin-coated beads
5. Pull off non-specifically bound beads
6. Detect remaining beads with GMR sensors

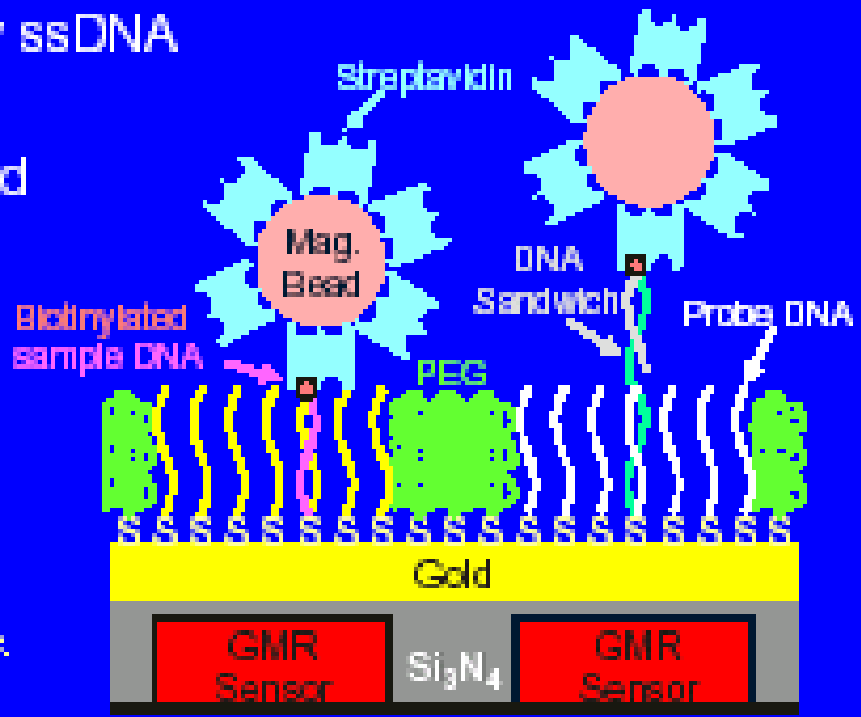

Edelstein, et al., Biosens. & Bioelec. 14, 805 (2000)

NVE

GMR / Fluidics Process Cross Section
Integration of fluidics and sensing

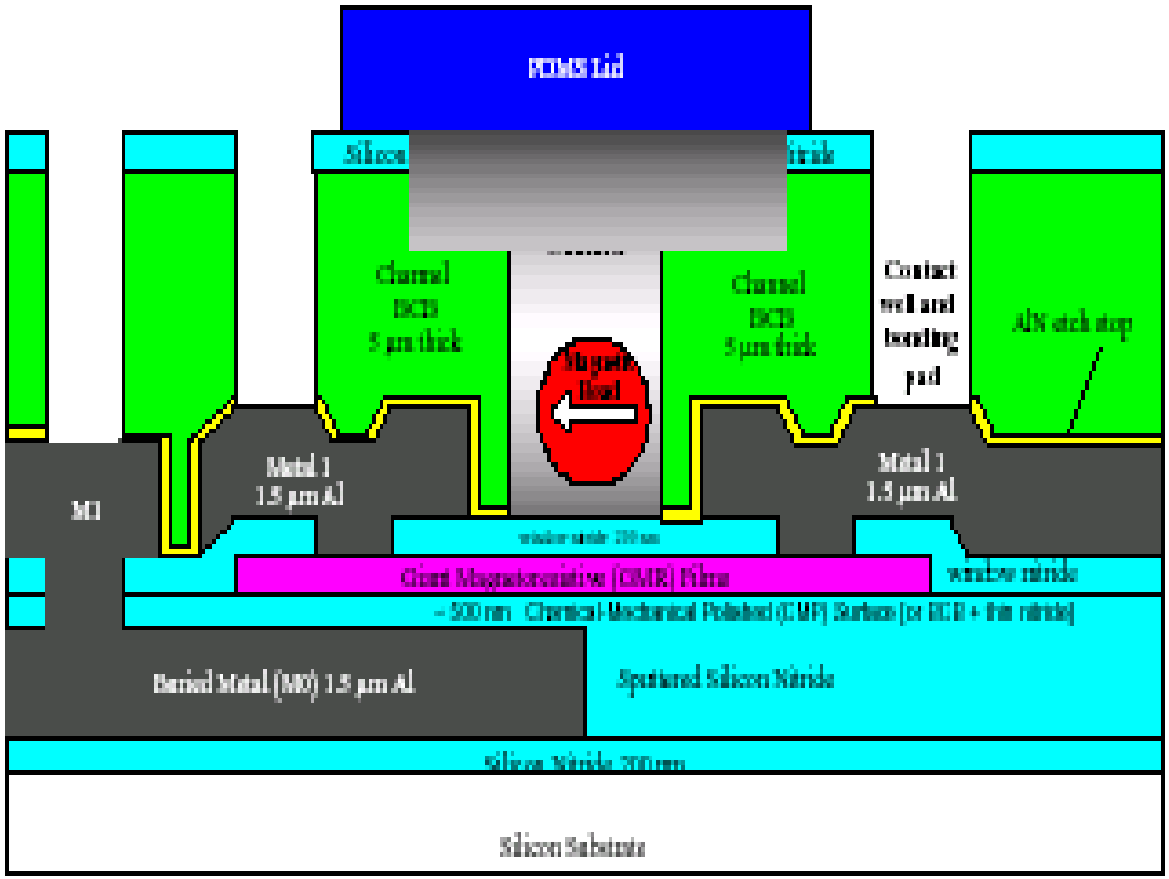

Cooperative Assembly of Magnetic Nanoparticles and Block Copolypeptides in Aqueous Media

*Larken E. Euliss†‡↔↩, Stephanie G. Grancharov†‡æ, Stephen O'Brien*æ, *Timothy J. Deming↔↩, Galen D. Stucky↔↩, C. B. Murray‡, G. A. Held*‡*

IBM TJ Watson Research Center, PO Box 218, Yorktown Heights, NY 10598, and Dept. of Applied Physics, Columbia University, New York, NY 10032, and Depts. of Chemistry and Materials Science, University of California, Santa Barbara, CA 93106

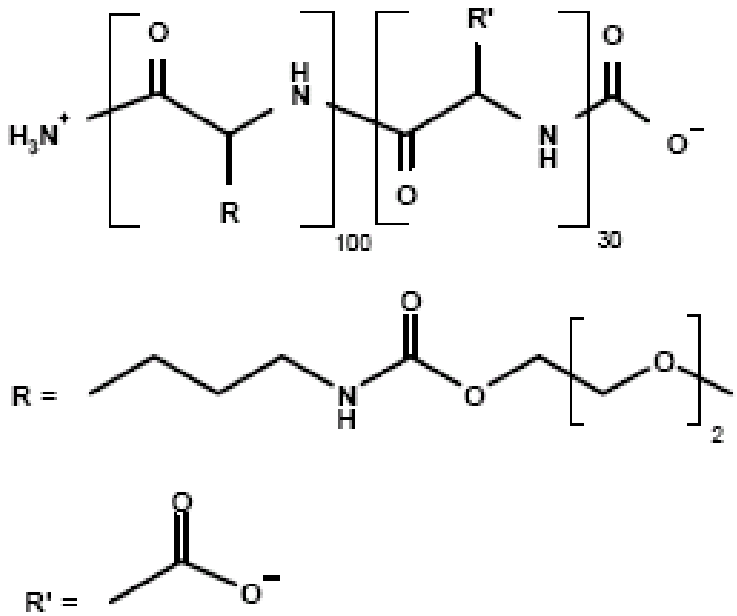

Figure 1. Molecular structure of block copolypeptide poly(diethyleneglycol functionalized-lysine)$_{100}$-poly(aspartic acid)$_{30}$ = poly(N_ε-2[2-(2-methoxyethoxy) ethoxy] acetyl-L-lysine)$_{100}$-β-poly (L-aspartic acid)$_{30}$.

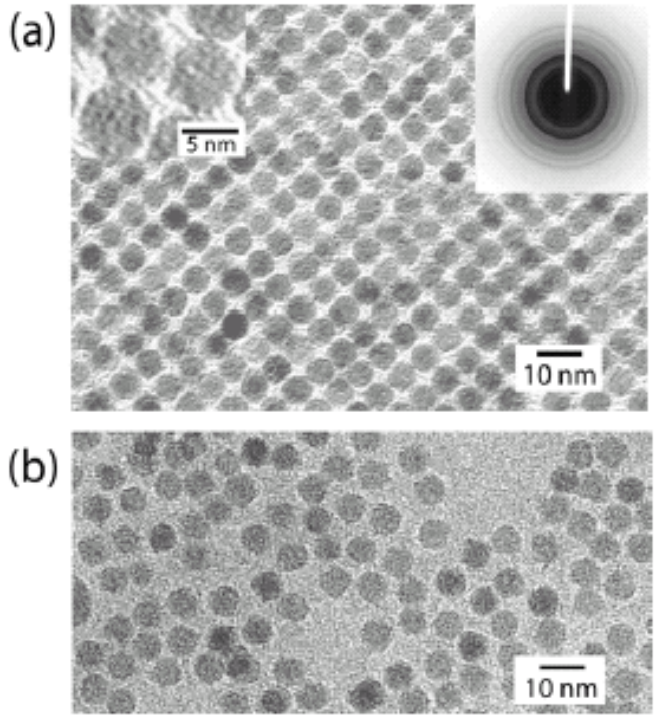

Figure 2. TEM micrographs of maghemite nanoparticles deposited from dispersions in (a) hexane and (b) water. Insets in (a) are a high resolution image of the nanoparticles and an electron diffraction pattern.

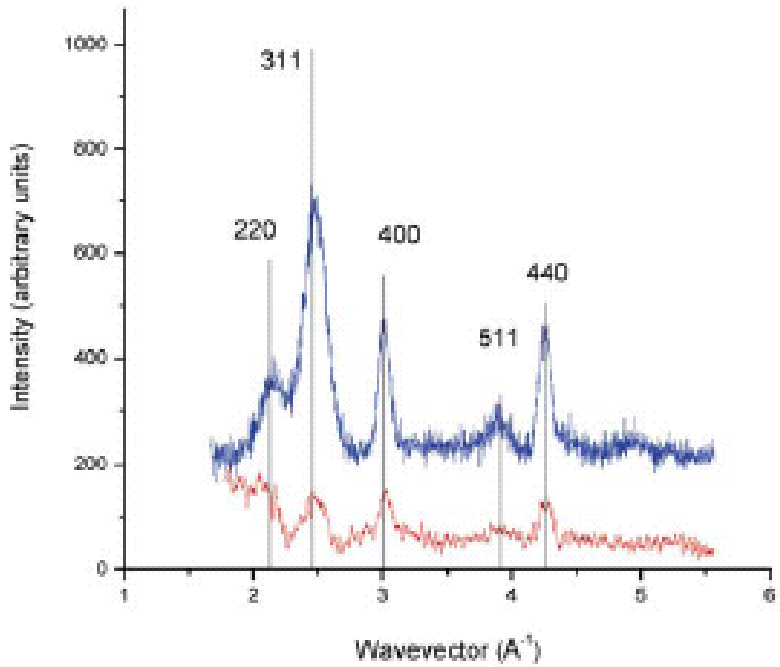

Figure 3. X-ray diffraction patterns of maghemite nanoparticles deposited onto glass substrates from dispersions in hexane (blue) and water (red). Intensity is plotted as a function of wavevector ($(4\pi/\lambda)\sin\theta$). Background has been subtracted from the red spectrum and the intensity of the blue

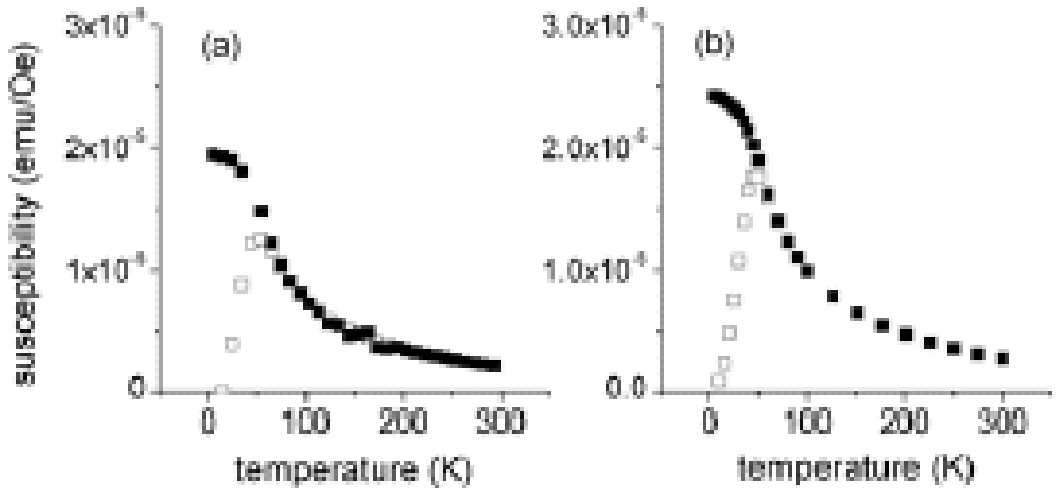

Figure 4. Low-field susceptibility as a function of temperature measured after zero-field cooling (□) and cooling in a 10 Oe field (■) measured for 6 nm maghemite nanoparticles deposited from dispersions in (a) hexane and (b) water. The field cooled and zero-field cooled scans for a given sample overlap at temperatures where the sample is in thermal equilibrium and diverge at the blocking temperature.

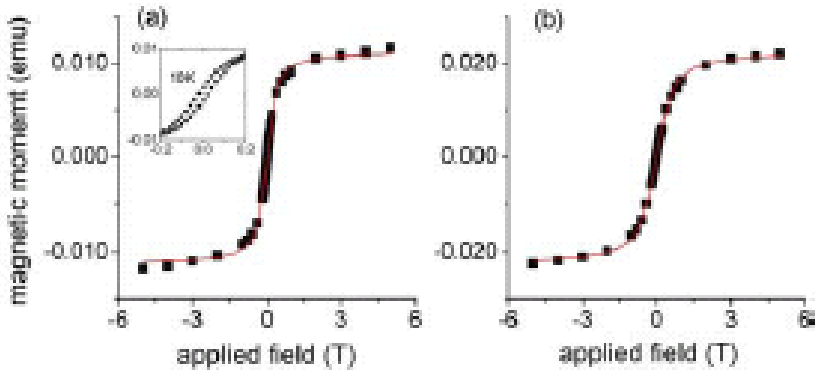

Figure 5. Magnetic moment as a function of applied magnetic field measured for 6 nm maghemite particles deposited from dispersions in (a) hexane and (b) water. Data were collected at 300K and (inset to (a)) 10K. Solid lines are best fits of the data to the Langevin paramagnetic function (see text).

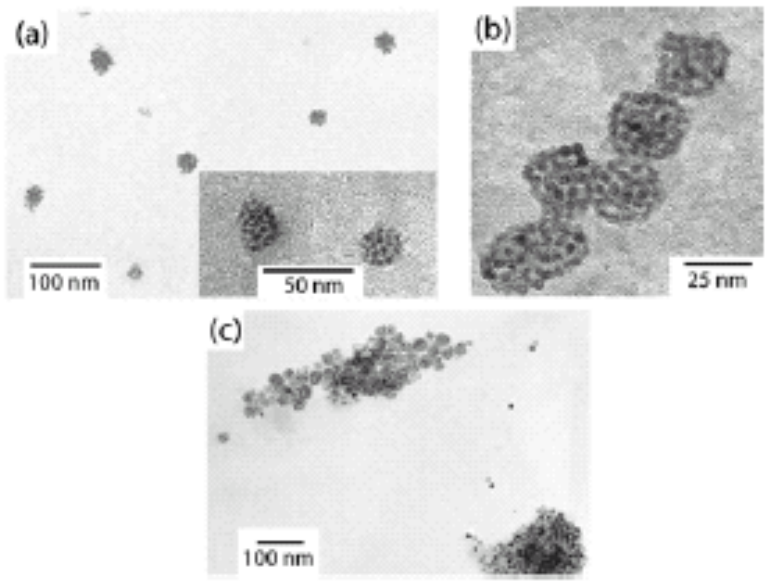

Figure 6. TEM micrographs of clusters of maghemite nanoparticles deposited from dispersions in water to which (a),(b) poly(diethyleneglycol functionalized-lysine)$_{100}$-poly(aspartic acid)$_{30}$ and (c) poly(aspartic acid)$_{30}$ have been added. Note that the homopolymer-nanoparticle mixture was not filtered prior to preparation of the TEM grid.

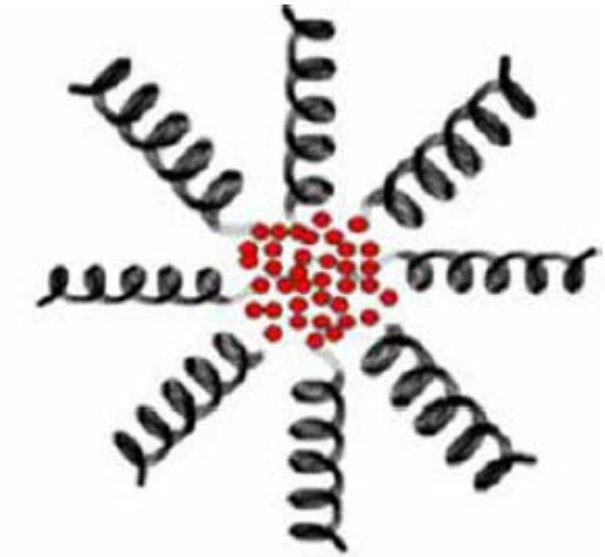

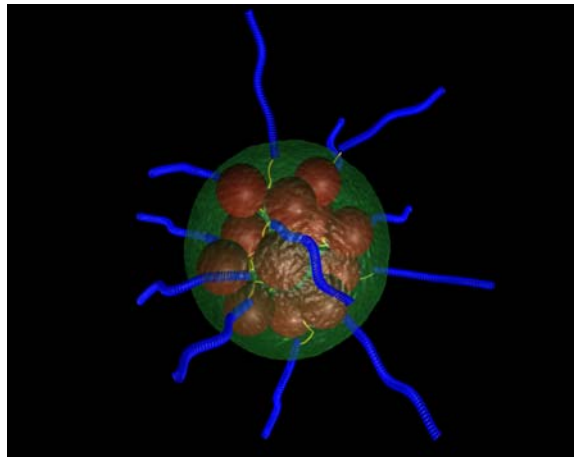

Figure 7. Schematic illustration of the proposed structure of the micelles formed following the addition of the block copolypeptide poly(diethyleneglycol functionalized-lysine)$_{100}$-poly(aspartic acid)$_{30}$ to an aqueous dispersion of 6 nm maghemite nanoparticles. The shell of the micelle is comprised of poly(diethyleneglycol functionalized-lysine)$_{100}$ which is known to form a stable α-helical conformation in water[10], while the core is comprised of maghemite nanoparticles bound to poly(aspartic acid)$_{30}$ chains.

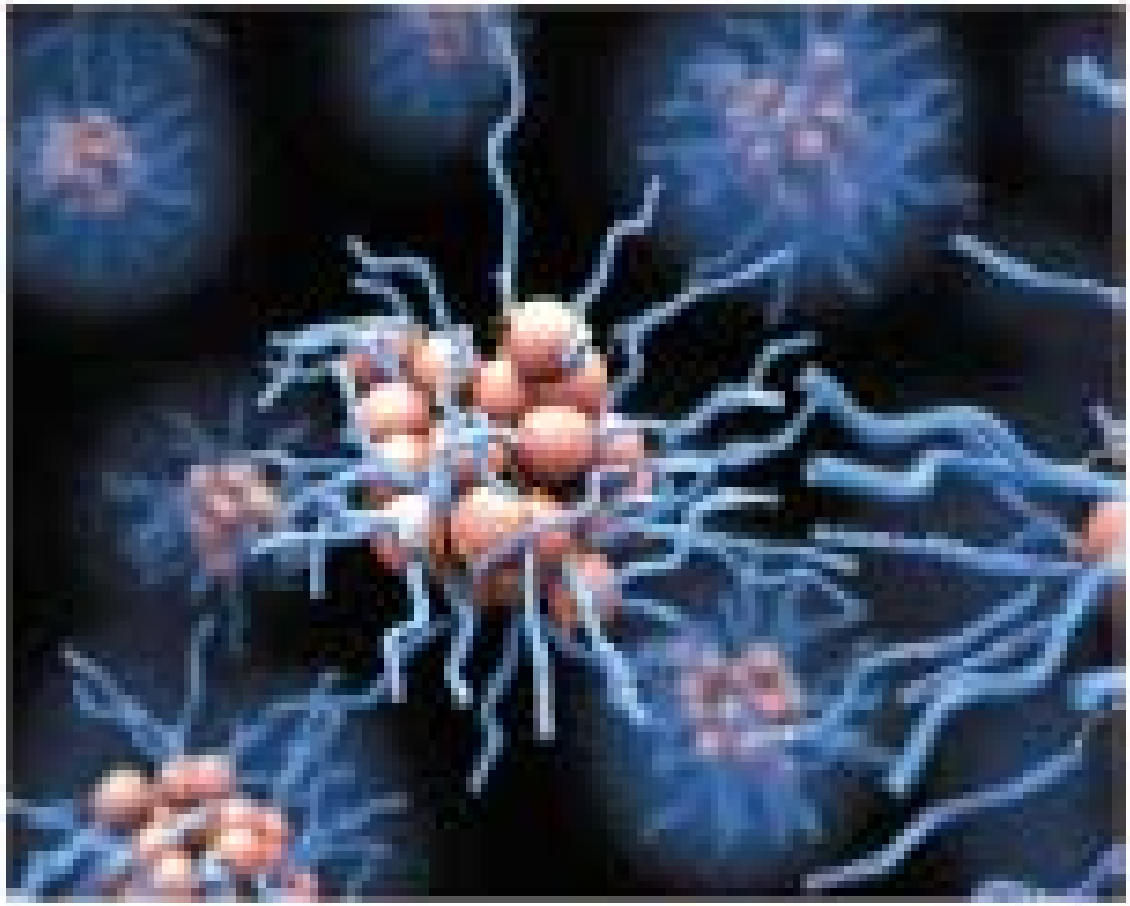

Chem. Mater. **1998**, *10*, 1021−1028

Spherical Assemblies of Semiconductor Nanoparticles in Water-Soluble Block Copolymer Aggregates

Matthew Moffitt,[†] H. Vali,[‡] and Adi Eisenberg*,[†]

Department of Chemistry, McGill University, 801 Sherbrooke Street West, Montreal, Q.C., Canada H3A 2K6, and Department of Earth and Planetary Sciences, McGill University, 3450 University Street, Montreal, Q.C., Canada H3A 2A7

Received August 1, 1997. Revised Manuscript Received January 30, 1998

Novel spherical assemblies of CdS-containing block copolymer reverse micelles in aqueous solution have been formed by the slow addition of water to mixtures of the reverse micelles and a polystyrene-*b*-poly(acrylic acid) stabilizer. The structures are large compound micelles (LCMs) with quantum-confined CdS nanoparticles dispersed throughout a spherical PS matrix, which is stabilized in water by a layer of solubilized hydrophilic chains. The size of the CdS particles ($2R_{CdS} \sim 3$ nm) is controlled by the ionic block length, N_B, of the block copolymer making up the reverse micelle. LCM formation is found to be dependent on the amount of added stabilizing copolymer. When the weight of stabilizer relative to the total polymer weight is 12% for the specific system under study, a single population of LCMs is formed ($D_{ave} = 64$ nm); each of these LCMs consists of an average of 58 reverse micelles and 87 stabilizing chains, with an average surface area per stabilizing chain of 148 nm.^{2} At 10% stabilizer, two LCM populations, $D_{ave} = 52$ nm and $D_{ave} = 152$ nm, are formed. When the concentration of stabilizing copolymer is increased to 21 and 35%, regular micelles with no internal structure coexist with LCMs. Without added stabilizing copolymer, most reverse micelles undergo macroscopic precipitation upon water addition, although some LCMs are observed in the remaining solution.

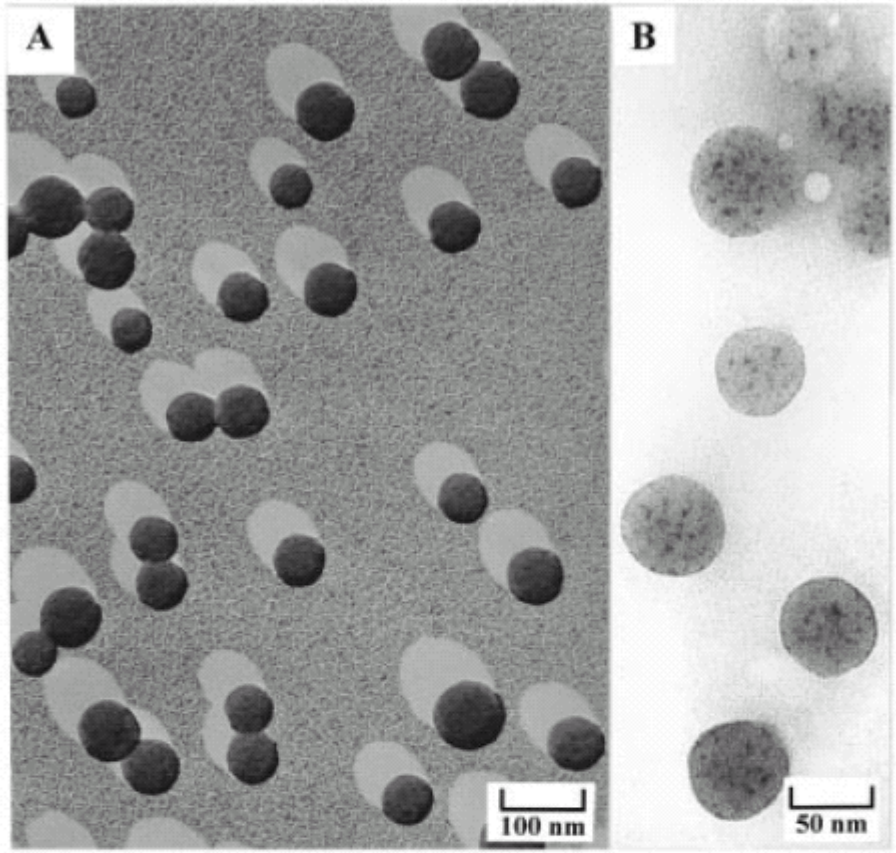

Figure 2. Transmission electron micrograph of spherical aggregates in LCM12, (A) with Pd/Pt shadowing and (B) without shadowing. The dark particles inside the spheres are CdS nanoparticles.

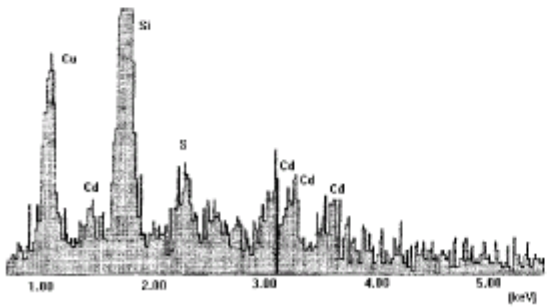

Figure 3. Energy-dispersive X-ray diffraction pattern of one of the aggregates containing dark particles, showing Cd and S bands.

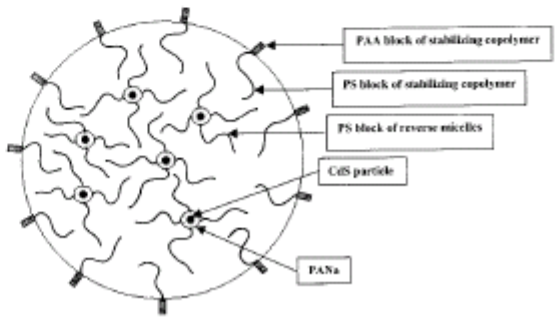

Figure 4. Schematic diagram of a large compound micelle containing CdS nanoparticles. The spherical aggregate is an assembly of reverse micelles, stabilized with added block copolymer.

at the surface of the LCM, minimizing interfacial